Hovering Control for Automatic Landing Operation of An Inspection Drone to A Mobile Platform

Li, Shaobao; Durdevic, Petar; Yang, Zhenyu

Published in:
IFAC-PapersOnLine

DOI (link to publication from Publisher):
10.1016/j.ifacol.2018.06.384

Publication date:
2018

Document Version
Publisher's PDF, also known as Version of record

Available online at www.sciencedirect.com

ScienceDirect

IFAC PapersOnline CONFERENCE PAPER ARCHIVE

IFAC PapersOnLine 51-8 (2018) 245–250

Hovering Control for Automatic Landing Operation of An Inspection Drone to A Mobile Platform

Shaobao Li, Petar Durdevic, Zhenyu Yang

Department of Energy Technology, Aalborg University, Esbjerg Campus, Niels Bohus Vej 8, Esbjerg, 6700, Denmark (e-mail: shl@et.aau.dk;pdl@et.aau.dk;yang@et.aau.dk).

Abstract: This paper investigates the hovering control problem of a drone on a 6-DOF mobile platform. An inner-outer loop strategy based on high-gain observer is presented. In the outer loop, the high-gain observer is designed to estimate the states of the drone such that its velocity and acceleration measurements are not necessary, and then a nested saturation controller is designed. In the inner loop, a hybrid controller which can be effectively used for avoiding unwinding phenomenon is applied to regulate the attitude of the drone. Finally, a simulation example is used to demonstrate the effectiveness of the proposed control method.

Keywords: Hovering, landing, high-gain observer, hybrid control, underactuated system.

1. INTRODUCTION

Drones have been widely applied for environment and production surveillance such as offshore oil & gas exploration and production, wind farm inspection, geography mapping, and so on (Schäfer et al. (2016); Lee et al. (2016)). Take the oil & gas production as an example. Drones have been applied to increase the effecitivity of areial inspection for facility integrity check, pollution monitoring, as well as facility/pipeline inspection etc. Drone is often operated remotely by professional operators from the platform or boats. However, to realize a smooth and safe landing of a commissioning drone on the moving deck is far more complicated, and there seems to us that there is no much study or development being found about automatic landing of drone on a moving platform either.

Similar to the manned aircrafts' landing on a mobile platform procedure, the automatic landing of a drone on a moving deck consists of two phases: hovering and landing. During hovering phase, drones need to track the 3D trajectory of the moving deck, keep a fixed height to the moving deck and adjust their attitudes properly for final landing. In this paper, we will focus on the hovering control of a drone. Normally, due to the functional controllability constraint of the drone, it cannot track the trajectory of the moving deck while keeping their attitudes matching. In recent years, some approaches have been developed to solve the similar hovering control problem. For example, Choi and Ahn (2015) studied the point tracking of a drone in 3D space and presented a backstepping-like feedback linearization method for control design. The proposed method is only designed for static position tracking. In (Serra et al. (2016)), a visual-servo-based control law was proposed for landing control of a drone on a moving target, where the high-gain inner-loop control is applied such that the attitude dynamcis are fast enough to neglect their affects on the outer-loop control, which is used to control the position of the drone. However, this method is usually not effective for large drones due to large inertia and input saturation. In (Tan et al. (2016)), an invariant ellipsoid-based method control law was proposed for hovering of a drone on a moving ship deck. Only the motion on heave of the ship is considered and attitude control is not studied. According to our survey, the existing approaches are still not effective for hovering and landing control of a drone on a 6-DOF moving deck. More recently, some methods based on inner-outer loop control strategy provide an inspiration for hovering control on a 6-DOF moving deck. Cao and Lynch (2016) presented an inner-outer loop control strategy for underactuated drone with input and state constraints, achieving globally asymptotically stable results for position and attitude tracking. Naldi et al. (2017) proposed a robust inner-outer loop control scheme for a drone with uncertain intertial matrix. However, the velocity and acceleration are required to be measurable in these two works. In most of low-cost drones, acceleration cannot be measured. Therefore, hovering control for drones without using velocity and acceleration measurements would be more desirable.

In this paper, we investigate the hovering control problem of a drone above a 6-DOF moving deck under disturbances. The control objective is to make the drone track the trajectory of the moving deck while achieving the best matching attitude between the drone and the deck while safisfying the functional controllability constraint. Towards this end, the mapping between the deck and the desired trajectory of the drone satisfying the functional controllability constraint is constructed, and then an inner-outer loop control scheme based on high-gain observer is employed for control development, where a nested saturation controller based on the high-gain observer is proposed for the outer loop control, and a hybrid control is applied for the inner-loop control to avoid unwinding phenomenon.

10.1016/j.ifacol.2018.06.384

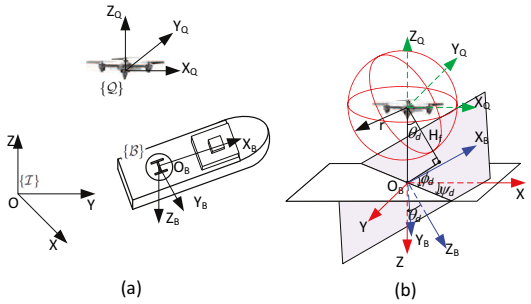

Fig. 1. Coordinate frames and hovering problem description

Notations: Throughout this paper, $\mathbf{R}$, $\mathbf{R}^m$ and $\mathbf{R}^{n\times m}$ denote the spaces of real numbers, real m-vectors and real $n \times m$ matrices, respectively. The terms $\|\cdot\|_p$ and $\|\cdot\|_\infty$ denote the p-norm and infinity norm, respectively.

2. PROBLEM FORMULATION

2.1 Dynamic Model of Drone

To describe the motion of a drone and a 6-DOF moving deck, three reference frames are defined as shown in Fig. 1(a): the inertial reference frame $\{\mathcal{I}\}$ fixed to the earth surface, the platform body-fixed frame $\{\mathcal{B}\}$ attached to the deck surface and the drone body-fixed frame $\{\mathcal{Q}\}$ attached to the drone's gravity center.

The drone is described by the following dynamic model:

$$\begin{aligned} \dot{p} &= v \\ M\dot{v} &= -u_f R e_3 + Mge_3 + d_f \\ \dot{R} &= RS(\omega) \\ J\dot{\omega} &= S(J\omega)\omega + u_\tau + d_\tau \end{aligned} \tag{1}$$

where $p = [x, y, z]^T \in \mathbf{R}^3$ and $v = [v_x, v_y, v_z]^T \in \mathbf{R}^3$ denote the position of the gravity center of the drone and its velocity in the inertial reference frame $\{\mathcal{I}\}$, respectively, $u_f \in \mathbf{R}$ is the scale translational control force, $u_\tau \in \mathbf{R}^3$ is the attitude control torque, $M > 0 \in \mathbf{R}$ and $J = J^T > 0 \in \mathbf{R}^{3\times3}$ are the mass and the inertia matrix of the drone, respectively, $d_f \in \mathbf{R}^3$ and $d_\tau \in \mathbf{R}^3$ are the bounded unknown disturbances, $g = 9.8$ is the acceleration of gravity, $e_3 = [0, 0, 1]^T$, $S(\cdot) \in \mathbf{R}^{3\times3}$ is a skew symmetric matrix regarding a vector $x = [x_1, x_2, x_3]^T \in \mathbf{R}^3$ given as

$$S(x) = \begin{bmatrix} 0 & -x_3 & x_2 \\ x_3 & 0 & -x_1 \\ -x_2 & x_1 & 0 \end{bmatrix}, \tag{2}$$

and $R \in SO(3)$ is the rotation matrix from $\{\mathcal{Q}\}$ to $\{\mathcal{I}\}$, where $SO(3)$ is the special orthogonal group of 3rd order:

$$SO(3) = \{R \in \mathbf{R}^{3\times3} : R^T R = RR^T = I_3, |R| = 1\}. \tag{3}$$

The element of $SO(3)$ can be parametrized by a unit quaternion as $q = \begin{bmatrix} \eta & \epsilon^T \end{bmatrix}^T$ through Rodrigues formula:

$$R(q) = I_3 + 2\eta S(\epsilon) + 2S(\epsilon)^2,$$

where $\eta \in \mathbf{R}$ and $\epsilon \in \mathbf{R}^3$ are the scalar and vector components of the unit quaternion q. See more details in (Shuster (1993)). Then the kinematic equation (the third equation of (1)) can be replaced by the following equation:

$$\dot{q} = \frac{1}{2} q \otimes \nu(\omega) = \frac{1}{2} \begin{bmatrix} -\epsilon^T \\ \eta I_3 + S(\epsilon) \end{bmatrix} \omega, \tag{4}$$

where $\nu(\omega) = \begin{bmatrix} 0 & \omega^T \end{bmatrix}^T$ and $\otimes$ is an operator between two quaternions $q_i = \begin{bmatrix} \eta_i & \epsilon_i^T \end{bmatrix}^T, i = 1, 2$, defined as follows:

$$q_1 \otimes q_2 = \begin{bmatrix} \eta_1 & -\epsilon_i^T \\ \epsilon_1 & \eta_1 I_3 + S(\epsilon_1) \end{bmatrix} \begin{bmatrix} \eta_2 \\ \epsilon_2 \end{bmatrix}.$$

2.2 Hovering Control Problem

This paper focuses on hovering control of a drone above a 6-DOF moving deck. We assume that the desired trajectory and attitude of the deck are determined by the nonlinear functions $p_d(t) = [x_d, y_d, z_d]^T \in \mathbf{R}^3$ and $\gamma_d(t) = [\phi_d, \theta_d, \psi_d]^T \in \mathbf{R}^3$ with respect to time t, respectively, where $p_d(t)$ and $\gamma_d(t)$ are 4th continuous differentiable. Therefore, we can define the velocity and angular velocity of the deck as $v_d(t) = \dot{p}_d$ and $w_d(t) = \dot{\gamma}_d$, respectively.

Hovering control aims at tracking the position of the moving deck and keeping a constant heaving distance to the deck. This process is very important for a drone landing on a moving deck safely. The most desirable control is that the controlled drone can track the deck while keeping the same attitude as that of the deck. However, it is noted that the second equation of (1) is underactuated, which means that as the drone flies along the desired trajectory p_d, its desired attitude R^* must satisfy the following functional controllability constraint by neglecting disturbance d_f:

$$R^* e_3 = \frac{Mge_3 - M\ddot{p}_d}{u_f}. \tag{5}$$

Obviously, the moblie platform has its own intrinsic attitude $R_d(\gamma_d)$ that usually cannot satisfy the constaint condition (5). Since position plays a major role in landing control, this paper will study how to make the drone track the position of the deck while achieving the best attitude matching.

To make the descent of the drone smooth, a descenting function $H(t)$ is defined. It is conveniently designed to be a smooth sigmoid function. An example will be given in Section 4. Denote $H_0 = H(t_0)$ be the initial height and $H_f = H(\infty)$ be the final height of the drone in the heave of the deck as shown in Fig. 1(b).

It is noted that, to keep the heaving distance H_f, the desired position z^* of the drone in the inertial frame needs to follow the following trajectory:

$$z^* = \frac{H_f}{\cos(\theta_d)} + z_d. \tag{6}$$

Therefore, the hovering control problem can be solved if the drone can track the desired trajectory p_d^* described as

$$p_d^* = p_d + H(t)e_3 + \frac{H_f e_3}{\cos(\theta_d)}. \tag{7}$$

while keeping an attitude satisfying the constraint (5).

3. HOVERING CONTROLLER DESIGN

In this section, an inner-outer loop control strategy will be introduced to design the hovering controller. The structure of the inner-outer loop control is shown in Fig. 2.

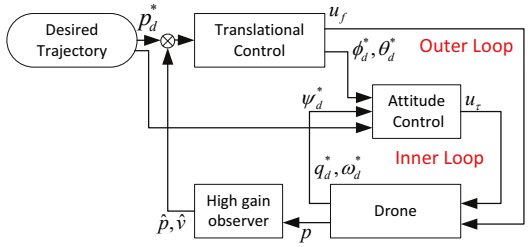

Fig. 2. Structure of Inner-Outer Loop Control

3.1 High-Gain Observer

The high-gain observer is introduced in the outer loop control because velocity and acceleration measurement may be unavailable for some low-cost drones. It is designed based on the following lemma:

Lemma 1. (Behtash (1990)). Consider a system with its output $y(t) \in \mathbf{R}^m$ and its first $n-1$ derivative being bounded, i.e., there are postive constants Y_k, $k = 1, \cdots, n-1$ such that $\|y^{(k)}\| < Y_k$. Given a high-gain observer

$$\begin{cases} \delta\dot{\xi}_i = \xi_{i+1}, \quad i = 1, \cdots, n-1 \\ \delta\dot{\xi}_n = -\lambda_1\xi_n - \lambda_2\xi_{n-1} - \cdots - \lambda_{n-1}\xi_2 - \xi_1 + y(t) \end{cases} \tag{8}$$

with δ being any small positive constant, ξ_i, $i = 1, \cdots, n$ being the observer states, and λ_i, $i = 1, \cdots, n-1$, being chosen such that the polynomial $s^n + \lambda_1 s^{n-1} + \cdots + \lambda_{n-1}s + 1$ is Hurwitz, then we have

1) $\frac{\xi_{k+1}}{\delta^k} - y^{(k)} = -\delta\Psi^{(k+1)}$, $k = 0, 1, \cdots, n-1$, where $\Psi = \xi_n + \lambda_1\xi_{n-1} + \cdots + \lambda_{n-1}\xi_1$.
2) There exist positive constants t^* and b_k, only depending on Y_k, $k = 1, \cdots, n$, δ and λ_i, $i = 1, \cdots, n-1$, such that $\|\Psi^{(k)}\| \le b_k$ for all $t > t^*$.

Obviously, Lemma 1 implies that $y^{(k)}$ can be estimated by $\frac{\xi_{k+1}}{\delta_k}$ bounded by δb_{k+1}, $k = 0, 1, \cdots, n-1$. It is noted that the high-gain observer does not need to know the system dynamics but only its output. This property has made the high-gain observer widely applied to estimate complex nonlinear systems.

In this paper, a high-gain based on Lemma 1 is designed to estimate the position and velocity of the drone under disturbances. The designed high-gain observer is given as follows:

$$\begin{cases} \delta\dot{\pi}_1 = \pi_2 \\ \delta\dot{\pi}_2 = -\lambda_1\pi_2 - \pi_1 + p \end{cases} \tag{9}$$

where $\pi_1, \pi_2 \in \mathbf{R}^3$ are the observer states. Choose λ_1 such that $s^2 + \lambda_1 s + 1$ is Hurwitz, and then the estimation of the position and velocity of the drone can be described as

$$\hat{p} = \pi_1 \tag{10}$$

$$\hat{v} = \frac{\pi_2}{\delta} \tag{11}$$

and there exist constants b_1 and b_2 such that

$$\|p - \hat{p}\| \le \delta b_1 \tag{12}$$

$$\|v - \hat{v}\| \le \delta b_2. \tag{13}$$

3.2 Translational Motion Control

Translational motion control aims at making the drone track the desired trajectory p_d^* such that the qudrotor can hover on the deck while keeping a desired heaving distance.

Recall the translational motion control design with velocity feedback in (Naldi et al. (2017)) first. Let

$$z_1 = p - p_d^*, \ z_2 = v - \dot{p}_d^*.$$

With the first two equations of (1), we have

$$\begin{cases} \dot{z}_1 = z_2 \\ M\dot{z}_2 = -u_f Re_3 + Mge_3 - M\ddot{p}_d^* + d_f \end{cases} \tag{14}$$

A vectored-thrust control strategy can be applied to design the scalar controller u_f. Define a control force vector $F_c(z_1, z_2)$ as follows:

$$F_c(z_1, z_2) = Mge_3 - M\ddot{p}_d^* + \kappa(z_1, z_2). \tag{15}$$

where $\kappa(z_1, z_2)$ is a state feedback law satisfying $\kappa(0, 0) = 0$.

Substituting (15) into the second equation of (14), we have

$$M\dot{z}_2 = -u_f Re_3 + F_c(z_1, z_2) - \kappa(z_1, z_2) + d_f. \tag{16}$$

We can define a desired attitude $R_c(z_1, z_2) \in SO(3)$ satisfying

$$u_f R_c e_3 = F_c(z_1, z_2).$$

Choose the translational motion control law as

$$u_f = \|F_c(z_1, z_2)\|. \tag{17}$$

Then, we have

$$R_c e_3 = \frac{F_c(z_1, z_2)}{\|F_c(z_1, z_2)\|}. \tag{18}$$

Then, system (14) can be rewritten as

$$\begin{cases} \dot{z}_1 = z_2 \\ M\dot{z}_2 = -u_f(R - R_c)e_3 - \kappa(z_1, z_2) + d_f. \end{cases} \tag{19}$$

A nested saturation function $\sigma(\cdot)$ can be used to design $\kappa(z_1, z_2)$ to meet the saturation requirement of the scalar control force u_f. According to (Naldi et al. (2017)), the following state feedback law is available to guarantee the stability of (19) under the scalar control (17).

$$\kappa(z_1, z_2) = \gamma_2\sigma\left(\frac{k_2}{\gamma_2}\left(z_2 + \lambda_1\sigma\left(\frac{k_1}{\gamma_1}z_1\right)\right)\right), \tag{20}$$

where k_1, k_2, γ_1, and γ_2 are some positive constants, and $\sigma(\cdot)$ is the saturation function satisfying the following properties for any $s \in \mathbf{R}$:

1) $|\dot{\sigma}(s)| \le 2$;
2) $|\ddot{\sigma}(s)| \le d$ for some $d > 0$;
3) $s\sigma(s) > 0$ for all $s \ne 0$, and $\sigma(0) = 0$;
4) $\sigma(s) = \mathrm{sgn}(s)$ for $|s| \ge 1$;
5) $|s| < |\sigma(s)| < 1$ for $|s| < 1$.

For a vector s, $\sigma(\cdot)$ is simply extended by each element satisfying the above properties. Note that each dimension of $\kappa(z_1, z_2)$ is bounded by γ_2.

Next, we will further discuss the translational motion control design independent of velocity and acceleration measurements. With the high-gain observer proposed in subsection 3.1, a new control law replacing the position and velocity by their estimates is designed as

$$\kappa'(\hat{z}_1, \hat{z}_2) = \gamma_2\sigma\left(\frac{k_2}{\gamma_2}\left(\hat{z}_2 + \gamma_1\sigma\left(\frac{k_1}{\gamma_1}\hat{z}_1\right)\right)\right), \tag{21}$$

where $\hat{z}_1 = \hat{p} - p_d^*$ and $\hat{z}_2 = \hat{v} - \dot{p}_d^*$. Then we can define a new control force vector $F_c'(\hat{z}_1, \hat{z}_2)$ as

$$F_c'(\hat{z}_1, \hat{z}_2) = Mge_3 - M\ddot{p}_d^* + \kappa'(\hat{z}_1, \hat{z}_2). \tag{22}$$

Let the translational motion control law in the form as

$$u'_f = \|F'_c(\hat{z}_1, \hat{z}_2)\|, \tag{23}$$

and the desired attitude R_c^* satisfying functional controllability constraint is given by

$$R_c^* e_3 = \frac{F'_c(\hat{z}_1, \hat{z}_2)}{\|F'_c(\hat{z}_1, \hat{z}_2)\|}. \tag{24}$$

With the new translational motion control law (23), system (19) is changed into

$$\begin{cases} \dot{z}_1 = z_2 \\ M\dot{z}_2 = -u'_f(R - R_c^*)e_3 - \kappa'(\hat{z}_1, \hat{z}_2) + d_f. \end{cases} \tag{25}$$

Then, we have the following results.

Theorem 2. Consider the drone system (1) tracking the desired trajectory p_d^* described in (7). Design a high-gain observer in the form of (9) with the ploynomial $s^2+\lambda_1 s+1$ being Hurwitz by choosing proper constant λ_1. Assume that there exists a constant $\chi^* > 0$ such that $\|u'_f(R - R_c^*)e_3\|_\infty \leq \chi^*$. Under the translational motion control law (23) with $\kappa'(\hat{z}_1, \hat{z}_2)$ and $F'_c(\hat{z}_1, \hat{z}_2)$ given in (21) and (22), respectively, and k_1, k_2, γ_1 and γ_2 satisfying

$$\frac{\gamma_2}{k_2} < \frac{\gamma_1}{4}, 4k_1\gamma_1 < \frac{\gamma_2}{4M}, \frac{144k_1}{k_2} < 1, \tag{26}$$

system (25) is ISS with respect to the input $-u'_f(R - R_c^*)e_3+d_f$, without restricions on the initial states and the input. In particular, the states of system (25) are bounded by the following asymptotic bound

$$\|z_1\|_p \leq \frac{6M}{k_1 k_2}\|v_2\|_p, \ \|z_2\|_p \leq \frac{3M}{k_2}\|v_2\|_p, \tag{27}$$

where $v_2 = (u'_f(R-R_c^*)e_3+(\kappa(z_1, z_2)-\kappa'(\hat{z}_1, \hat{z}_2))+d_f)/M$.

Proof. Rewrite (25) in the form as

$$\begin{cases} \dot{z}_1 = z_2 \\ M\dot{z}_2 = -\kappa(z_1, z_2) - u'_f(R - R_c^*)e_3 \\ \qquad +(\kappa(z_1, z_2) - \kappa'(\hat{z}_1, \hat{z}_2)) + d_f \end{cases} \tag{28}$$

Let $\chi(R, R_c^*) = -u'_f(R-R_c^*)e_3$. System (28) can be viewed as a special case of system (C.1) in Appx C of (Isidori et al. (2012)) with $n = 2$, $q_1(t) = 1$, $q_2(t) = \frac{1}{M}$, $v_1 = 0$ and $v_2 = (\chi(R, R_c^*) + (\kappa(z_1, z_2) - \kappa'(\hat{z}_1, \hat{z}_2)) + d_f)/M$.

It is noted that the inequalities (12) and (13) imply that there exists a constant $\kappa^* > 0$ such that $\|\kappa(z_1, z_2) - \kappa'(\hat{z}_1, \hat{z}_2)\|_\infty \leq \kappa^*$. Therefore, there exists a constant $v_2^* > 0$ such that $\|v_2\|_\infty \leq v_2^*$.

Directly using the Lemma C.2.1 in (Isidori et al. (2012)), this theorem can be proved.

3.3 Attitude Control

In order to satisfy $\|\chi(R, R_c^*)\|_\infty \leq \chi^*$, an attitude control will be designed to make R track R_c^*. Note that the rotation matrix R_c^* is a mapping $[\phi_c^*, \theta_c^*, \psi_c^*]^T \to R_c^*$, and have the relationship described in XYZ convention as shown in (30). Therefore, through (24) we can fix ψ_c^* and θ_c^*. ψ_c^* can be chosen randomly, but in order to achieve the best matching attitude with the deck, the thrid Euler angle of the desired attitude is fixed by $\psi_c^* = \psi_d$. In this way, the desired attitude of the drone is determined, and the quaternion q_c^* corresponding to R_c^* can be obtained based on the quaternion algebra (Shuster (1993)).

Based on the third equation of (1), the desired angular velocity ω_c^* corresponding to R_c^* is calculated by

$$\omega_c^* = GR_c^{*T}\dot{R}_c^* e_3 + \dot{\psi}_d e_3,$$

where G is the matrix with the first, second and third rows given by $[0, -1, 0]$, $[1, 0, 0]$ and $[0, 0, 0]$, respectively, and $\dot{\psi}_d$ is the angular velocity of the deck in yaw.

Define the quanternion error $\tilde{q}$ and the angular velocity error $\tilde{\omega}$ as

$$\tilde{q} = q_c^{*-1} \otimes q \tag{31}$$

$$\tilde{\omega}_c = \omega - \bar{\omega}_c, \tag{32}$$

where $\bar{\omega}_c = R(\tilde{q})^T\omega_c^*$. Then, the attitude error system can be written as

$$\begin{cases} \dot{\tilde{q}} = \frac{1}{2}\tilde{q} \otimes \begin{bmatrix} 0 \\ \tilde{w}_c \end{bmatrix} \\ J\dot{\tilde{\omega}}_c = \Lambda(\tilde{\omega}_c, \bar{\omega}_c)\tilde{\omega}_c + S(J\bar{\omega}_c)\bar{\omega}_c - JR(\tilde{q})^T\dot{\omega}_c^* + u_\tau + d_\tau \end{cases} \tag{33}$$

with $\Lambda(\tilde{\omega}_c, \bar{\omega}_c)$ defined as

$$\Lambda(\tilde{\omega}_c, \bar{\omega}_c) = S(J\tilde{\omega}_c) + S(J\bar{\omega}_c) - S(\bar{\omega}_c)J - JS(\bar{\omega}_c).$$

Remark 3. $\tilde{q} = [\pm 1, 0, 0, 0]^T$ are both the equilibriums of the first equation of (33), because $\tilde{q} = [\pm 1, 0, 0, 0]^T$ denote the same attitude in the 3D space.

Referring to the hybrid control method proposed in (Mayhew et al. (2011)), the attitude control law is designed as

$$u_\tau = JR(\tilde{q})^T\dot{\omega}_c^* - S(J\bar{\omega}_c)\bar{\omega}_c - k_3 h\tilde{\epsilon} - k_4\tilde{\omega}_c, \tag{34}$$

where $\tilde{\epsilon}$ is the vector component of $\tilde{q}$, k_3 and k_4 are postive constants, and $h \in \{-1, 1\}$ is a variable governed by

$$\begin{cases} \dot{h} = 0, & h\tilde{\eta} > -\zeta \\ h^+ \in \overline{\text{sgn}}(\tilde{\eta}), & h\tilde{\eta} \leq -\zeta \end{cases} \tag{35}$$

where $\tilde{\eta}$ is the scalar of $\tilde{q}$, $\zeta \in (0, 1)$ is the hysteresis threshold, and $\overline{\text{sgn}}(\tilde{\eta})$ is defined as

$$\overline{\text{sgn}}(\tilde{\eta}) = \begin{cases} \text{sgn}(\tilde{\eta}), & |\tilde{\eta}| > 0 \\ \{-1, 1\}, & \tilde{\eta} = 0. \end{cases}$$

The attitude control law (34) is effective to handle the unwinding phenomenon (Bhat and Bernstein (2000)) and noise induced chattering (Mayhew et al. (2011)).

Then, we have the following theorem:

Theorem 4. Given the attitude error system (33), under the control law (34), system state $\tilde{x} = [\tilde{q}^T, \tilde{\omega}_c^T, h]^T$ is globally uniformly ultimately bounded. In particular, if $d_\tau \equiv 0$, system (33) is asymptotically stable.

Remark 5. Equation (24) implies $\dot{R}_c^* e_3 = \frac{d}{dt}\frac{F'_c(\hat{z}_1, \hat{z}_2)}{|F'_c(\hat{z}_1, \hat{z}_2)|}$. Then, $\dot{\omega}_c^*$ is computed by

$$\begin{aligned} \dot{\omega}_c^* &= G\dot{R}_c^{*T}\dot{R}_c^* e_3 + GR_c^{*T}\ddot{R}_c^* e_3 + \ddot{\psi}_d e_3 \\ &= GS(\omega_c^*)^T R_c^{*T}\frac{d}{dt}\frac{F'_c(\hat{z}_1, \hat{z}_2)}{|F'_c(\hat{z}_1, \hat{z}_2)|} + G\frac{d^2}{dt^2}\frac{F'_c(\hat{z}_1, \hat{z}_2)}{|F'_c(\hat{z}_1, \hat{z}_2)|} + \ddot{\psi}_d e_3. \end{aligned}$$

3.4 Stability of the Closed-Loop System

Combing Theorem 2 and Theorem 4, we can further obtain the stability of the whole closed-loop control system.

Theorem 6. Consider the drone system (1) and the desired trajectory p_d^* described in (7). Under the scalar translational motion controller (21) with γ_1, γ_2, k_1 and k_2

$$R_c^* = \begin{bmatrix} \cos(\theta_c^*)\cos(\psi_c^*) & -\cos(\theta_c^*)\sin(\psi_c^*) & \sin(\theta_c^*) \\ \cos(\phi_c^*)\sin(\psi_c^*) + \cos(\psi_c^*)\sin(\phi_c^*)\sin(\theta_c^*) & \cos(\phi_c^*)\cos(\psi_c^*) - \sin(\phi_c^*)\sin(\theta_c^*)\sin(\psi_c^*) & -\cos(\theta_c^*)\sin(\phi_c^*) \\ \sin(\phi_c^*)\sin(\psi_c^*) - \cos(\phi_c^*)\cos(\psi_c^*)\sin(\theta_c^*) & \cos(\psi_c^*)\sin(\phi_c^*) + \cos(\phi_c^*)\sin(\theta_c^*)\sin(\psi_c^*) & \cos(\phi_c^*)\cos(\theta_c^*) \end{bmatrix} \quad (30)$$

satisfying (26), and the attitude controller (34) with $k_3 > 0$ and $k_4 > 0$, the tracking errors z_1, z_2, $\tilde{q}$ and $\tilde{\omega}_c$ are globally uniformly ultimately bounded.

This theorem is obviously based on the ISS property in Theorem 2 and the globally uniformly ultimately bounded property in Theorem 4, and thus the proof is omitted here.

Remark 7. It can be observed from Theorem 2 and Theorem 4 that the tracking errors are dependent on d_f, d_τ and the estimation errors of the high-gain observer. Since small δ can enhance the accuracy of the high-gain observer, the tracking errors of the drone can also mitigated by choosing small δ.

4. SIMULATION STUDIES

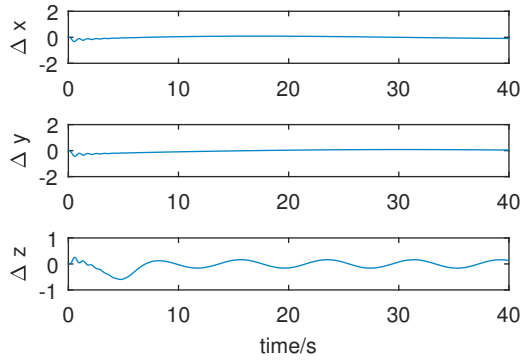

Fig. 3. The position estimation error of the high-gain observer.

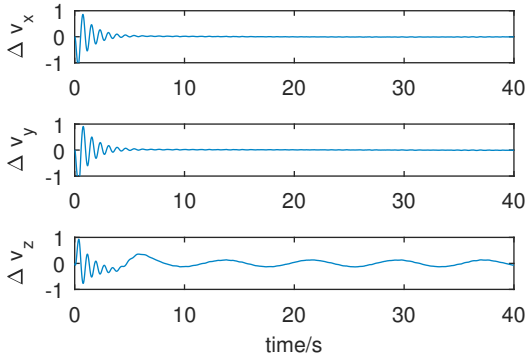

Fig. 4. The velocity estimation error of the high-gain observer.

In this section, a numerical example is presented to verify the effectiveness of the proposed control solution. The dynamic model of the drone is given by (1) with system parameters: $M = 3.25$kg, $J = \mathrm{diag}(0.032, 0.032, 0.164)$, and d_f and d_τ being the Gaussian white noises with maximum aplitude of 1.5N and 0.05Nm, respectively.

The position trajectory and Euler angles of the 6-DOF deck follow the following nonlinear functions:

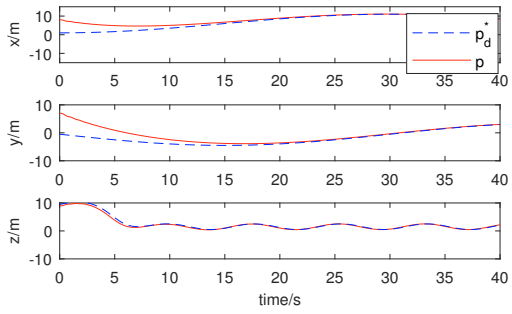

Fig. 5. The position trajectory of the drone.

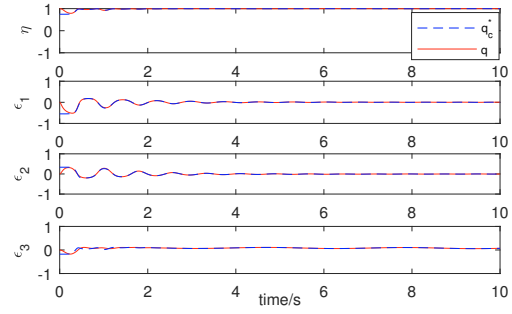

Fig. 6. The attitude trajectory of the drone.

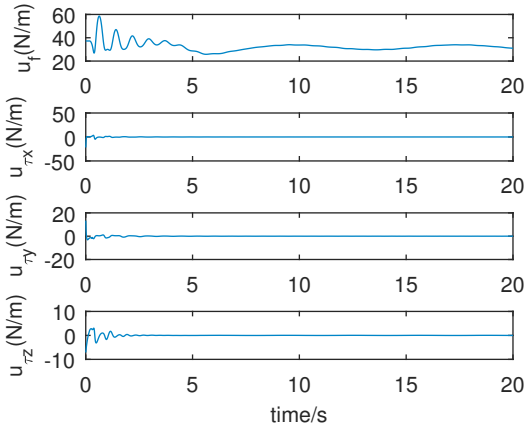

Fig. 7. The translational motion control force and attitude control torques of the drone.

$$p_d(t) = \begin{bmatrix} 6 - 5\cos(\frac{\pi}{30}t) \\ -0.5 - 4\sin(\frac{\pi}{30}t) \\ \sin(0.8t) \end{bmatrix}, \gamma_d(t) = 0.05 \begin{bmatrix} -\cos(2t) \\ \sin(2t) \\ -\cos(2t) \end{bmatrix},$$

respectively. The descending function $H(t)$ is defined as

$$H(t) = H_0 + \frac{H_f - H_0}{1 + e^{\frac{-6(2t-10)}{10}}}, \quad (36)$$

where, the initial height H_0 of the drone is determined by its initial position in Z axis. The drone is desired to hover at the height $H_f = 1$m above the deck. Then, the desired position trajectory p_d^* in (7) is obtained.

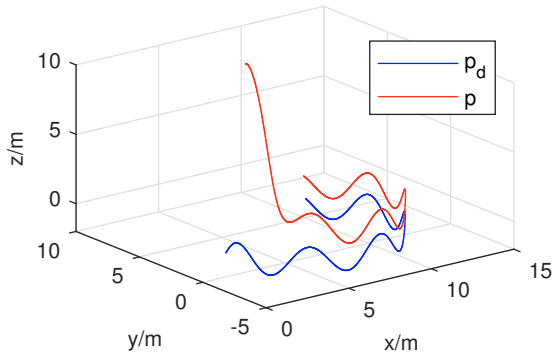

Fig. 8. The tracking trajectory of the drone in 3D.

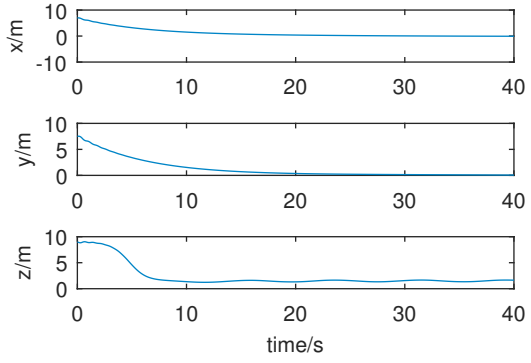

Fig. 9. The tracking errors of the drone.

The parameters of the high-gain observer (9), the control force (21) and the control torques (34) are given as: $\delta = 0.1$, $\lambda_1 = 2$, $k_1 = 0.1$, $k_2 = 26$, $\gamma_1 = 0.5$, $\gamma_2 = 26$, $k_3 = 40$ and $k_4 = 2$.

Simulation results are shown in Figures 3-9. Figures 3 and 4 show the position estimation error and velocity estimation error of the high-gain observer, respectively. It is observed that the estimation errors are very small and thus the designed high-gain observer is effective. In Figure 5, the blue dash line denotes the desired trajectory p_d^* and the red line is the trajectory of the drone. It is observed that the drone tracks the desired trajectory with very small tracking errors. Figure 6 illustates that the attitude of the drone tracks the desired attitude q_c^*. Figure 7 shows that the control force u_f and the control torques u_τ are bounded. In Figure 8, the blue line denotes the trajectory of the deck and the red line is the trajectory of the drone. From Figure 8 as well as Figure 9, it is observed that the drone tracks the moving deck while keeping an approximate height $H_f = 1$m above the deck. In summary, the simulation results demonstrate the effectiveness of the proposed control solution.

5. CONCLUSION

This paper studies the hovering problem of a drone above a 6-DOF moving deck. A high-gain observer is designed to estimate the position and velocity of the drone. Then, a nested saturation control is designed based on the high-gain observer to make the drone track the trajectory of the deck and keep a fixed heaving distance above the moving deck. A hybrid control is applied to make the attitude of the drone achieve the best matching with the attitude of the deck while satisfying the functional controllability constraint of the drone. The hybrid control is also available to aviod the unwinding phenomenon. The stability of the whole closed-loop system is theoretically proved. In the future, it would be interesting to further investigate visual based landing control of a drone on a moving deck and make an implementation on a practical drone.

ACKNOWLEDGEMENTS

This work is partially supported by the National Natural Science Foundation of P. R. China under Grant 61403334 and the Natural Science Foundation of Hebei Province under Grant F2017203109.

REFERENCES

Behtash, S. (1990). Robust output tracking for non-linear systems. *International Journal of Control*, 51(6), 1381–1407.

Bhat, S.P. and Bernstein, D.S. (2000). A topological obstruction to continuous global stabilization of rotational motion and the unwinding phenomenon. *Systems & Control Letters*, 39(1), 63–70.

Cao, N. and Lynch, A.F. (2016). Inner–outer loop control for quadrotor uavs with input and state constraints. *IEEE Transactions on Control Systems Technology*, 24(5), 1797–1804.

Choi, Y.C. and Ahn, H.S. (2015). Nonlinear control of quadrotor for point tracking: Actual implementation and experimental tests. *IEEE/ASME transactions on mechatronics*, 20(3), 1179–1192.

Isidori, A., Marconi, L., and Serrani, A. (2012). *Robust autonomous guidance: an internal model approach*. Springer Science & Business Media.

Lee, H., Hwang, Y.S., Jang, G., Kim, T., and Lee, J.M. (2016). 3d map building using the lrf and sinusoidal trajectory of a quadrotor. In *Robotics and Biomimetics (ROBIO), 2016 IEEE International Conference on*, 690–695. IEEE.

Mayhew, C.G., Sanfelice, R.G., and Teel, A.R. (2011). Quaternion-based hybrid control for robust global attitude tracking. *IEEE Transactions on Automatic Control*, 56(11), 2555–2566.

Naldi, R., Furci, M., Sanfelice, R.G., and Marconi, L. (2017). Robust global trajectory tracking for underactuated vtol aerial vehicles using inner-outer loop control paradigms. *IEEE Transactions on Automatic Control*, 62(1), 97–112.

Schäfer, B.E., Picchi, D., Engelhardt, T., and Abel, D. (2016). Multicopter unmanned aerial vehicle for automated inspection of wind turbines. In *Control and Automation (MED), 2016 24th Mediterranean Conference on*, 244–249. IEEE.

Serra, P., Cunha, R., Hamel, T., Cabecinhas, D., and Silvestre, C. (2016). Landing of a quadrotor on a moving target using dynamic image-based visual servo control. *IEEE Transactions on Robotics*, 32(6), 1524–1535.

Shuster, M.D. (1993). A survey of attitude representations. *Navigation*, 8(9), 439–517.

Tan, C.K., Wang, J., Paw, Y.C., and Liao, F. (2016). Autonomous ship deck landing of a quadrotor using invariant ellipsoid method. *IEEE Transactions on Aerospace and Electronic Systems*, 52(2), 891–903.